International Journal Of
Industrial Electronics Control and Optimization
Print ISSN: 3517-2645
Online ISSN: 3568-2645
Homepage: https://ieco.usb.ac.ir/

Adaptive Input-Output Feedback Linearization Control For Islanded Inverter-Based Microgrids

Navid Reza Abjadi[1]

Faculty of Engineering, Shahrekord University. Shahrekord, Iran.[1]
Corresponding author's email: abjadi.navidreza@sku.ac.ir, navidabjadi@yahoo.com

Article Info

Article type:
Research Article

Article history:
Received: 16-February-2023
Received in revised form: 21-July-2023
Accepted: 16-Aug-2023
Published online: 25-Aug-2023

Keywords:
Adaptive control,
Distributed generation,
Feedback linearization,
Master-slave strategy,
Microgrid.

ABSTRACT

Due to the growth of renewable energies and the need for sustainable electrical energy, AC microgrids (MGs) have been the subject of intense research. Medium voltage MGs will soon have a special place in the power industry. This paper uses a new and effective control scheme for islanded inverter-based medium voltage MGs using the master-slave (MS) technique. The controllers only need local measurements. The designed controls are based on adaptive input-output feedback linearization control (AIOFLC). These controls have a high-performance response, and are robust against some uncertainties and disturbances. The use of the designed control scheme makes the output voltage of distributed generation (DG) sources have negligible harmonics. Besides, the generated voltage and active/reactive powers track their references effectively. The model of the inverter-based DGs is considered in a stationary reference frame, and there is no need for any coordinate frame transformation. The control method presented in this paper can be used for MGs with any number of inverter-based DGs and parallel inverters. The effectiveness of the proposed control scheme is evaluated by simulation in SIMULINK/MATLAB environment and compared with that of feedback linearization control (FLC) and conventional sliding mode control (CSMC).

I. Introduction

Today, the severe warming of the earth due to greenhouse gases and environmental pollution endangered human lives in some areas, leading to the desire of many countries to be independent of fossil fuels. Accordingly, many efforts have been made to produce electricity from renewable energies such as wind and sun. One of the best ways to exploit these energy sources is to use them in the MG. The MG may be connected to the grid or disconnected from the grid. When MG is disconnected from the grid, it is called an islanded MG, wherein the voltage and frequency must be controlled and the required power must be divided between the DG sources. An islanded MG is a complicated multivariable system with difficult high performance control of voltage amplitude, frequency and active/reactive powers.

In an islanded MG, two types of strategies to share active/reactive powers between DGs are communication-free and communication-based strategies [1]. The droop control strategy is known as a communication-free strategy because it

requires local measurements [2]; however, this strategy is based on small signal models, which may cause instability in large signal changes. In addition, it causes DC bus voltage deviation [3]. In [4], proportional resonance (PR) control with a droop control strategy is used for an islanded MG. PR control is not robust against uncertainties, disturbances, and operating point changes. The well-known communication-based strategies are the centralized control strategy, distributed control strategy, and MS strategy [5]. Centralized control has a very good dynamic response but needs all of the information and measurements of the DGs, which may be far from each other such that the whole system may fail with a small defect [6]. In addition, it requires a high-speed expensive telecommunication. A low bandwidth link is needed for distributed control and MS strategy; since they need less MG data. MS strategy can result in excellent power sharing and is easily implemented [1].

In the MS strategy, the DG with the largest power capacity is called the master unit (MU), and the other DGs are called the slave units (SU). The MU controls the voltage and frequency of the MG, and the SUs control their active and reactive power output [1]. In [7], power sharing in MS strategy is investigated. In [8], a two-level control for MS strategy is designed which does not have a good dynamic response and does not work well in the face of disturbances and uncertainties. In [1], by adopting the MS strategy and proportional-integral (PI) control, the result of communication delay is investigated for two parallel inverters. Tuning the PI controllers depends on the operating points, and the method is not robust. In [9], a communication-free MS strategy is proposed for an MG. In this strategy, the MU is a synchronous generator and the SUs are current source inverters (CSIs).

In [10], the effect of coefficients of conventional decoupling PI in MS strategy is studied. In [11], a cascaded PI-based control is analyzed using the MS strategy in islanded MG**.** In [12], μ synthesis is used for MG with MS strategy. The DGs in [12] use a three-stage solid-state transformer with a complicated structure. In [13], adopting MS strategy, an H_∞ controller is proposed for the MU. However, for the SUs, PI controllers are used in the dq reference frame. Therefore, the overall closed-loop system is not robust. In addition, the design procedure of the H_∞ controller has several steps, and matrix manipulations are needed.

In [14], a nonlinear backstepping control is designed for an MG with MS strategy, which needs loads measurements. Backstepping control in [14] is a recursive method with many steps and is not robust.

CSMC is a method that has attracted such attention regarding its simple implementation and robustness. The main problem of CSMC is the chattering phenomenon. In [15]. adaptive SMC and adaptive feedback linearization methods are used for an MG with MS strategy. Given that there is no guarantee for the convergence of estimates to real values, the amount of control effort can be high, and instability may occur. In addition, the lumped uncertainties considered in the proposed control design in [16] are considered constants, while they are not constant. In fact, these lumped uncertainties depend on voltages, currents, and parameters uncertainties. In [16], the voltages and currents of an MG are controlled using high-order SMC methods by accepting centralized control strategy. The control scheme proposed in [16] is rather complex and it must be redesigned with the change of MG completely.

In [17], a secondary control method is used for a hybrid droop and MS structure. The control scheme of [17] requires internal current control loops, several abc/dq conversions, and too many parameters. In addition, it is not robust.

Model predictive control design for MS inverters is presented in [18]. In this paper, it is claimed that the controllers are robust with respect to uncertainties, while the obtained models are dependent on system parameters to predict voltages and currents.

A new enhanced droop control for MGs based on small signal models is proposed in [19]. Large disturbances and variations may cause instability in the overall proposed system.

In [20], an enhanced state feedback for secondary control in an islanded MG is designed. The control method of [20] is not robust with respect to MG parameters uncertainties.

Nonsingular terminal Sliding mode control (TSMC) is used for Islanded inverter-based MGs in [21]. A high-performance control scheme is achieved in [21]; however, fractional order calculation in TSMC causes difficulties in real time implementation especially when low-cost microcontrollers are used.

Adaptive feedback linearization control is a robust control. In [22], an AIOFLC is designed for a grid-connected inverter with an L filter to control the active and reactive powers injected into the grid.

This paper designs novel controls for inverter-based DGs of islanded MGs considering MS strategy. The inverters filters are LC filters and the applied control technique is AIOFLC. The modeling equations of MU and SUs are rewritten to suitable forms for AIOFLC. An AIOFLC is designed for MU to control the voltage of the MU bus. Another AIOFLC is designed for SUs to control the active and reactive powers delivered by SUs. There is symmetry in the control design because the AIOFLCs are designed for both master and slave units. Using the proposed control method, a high-performance closed–loop control system is achieved. The stability is guaranteed. The microgrid handles the load switching, uncertainties and disturbances properly. Several case studies are investigated and the simulation results are represented.

II. MG configuration and modeling

The islanded MG investigated in this paper is given in Fig 1a.

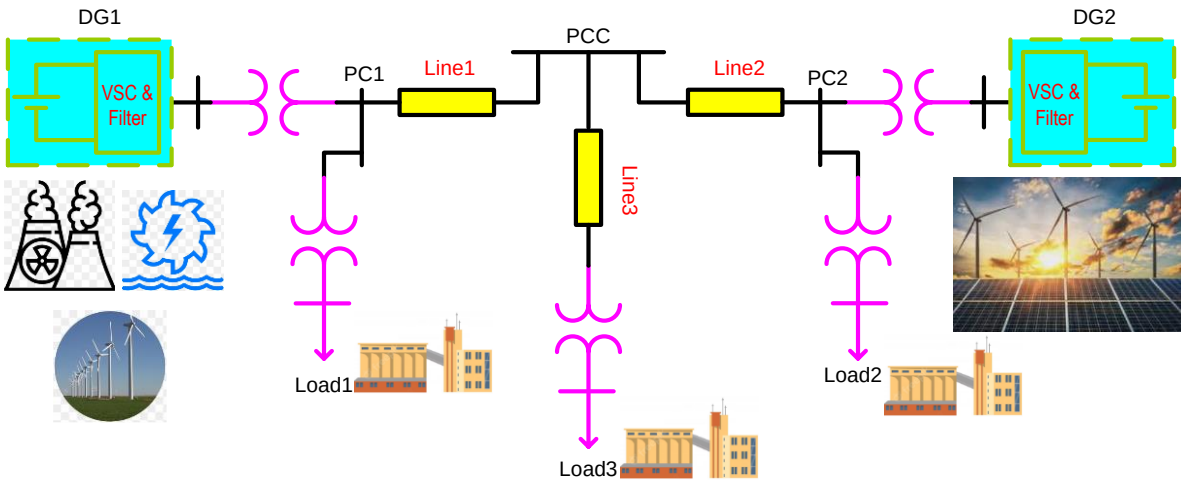

(a)

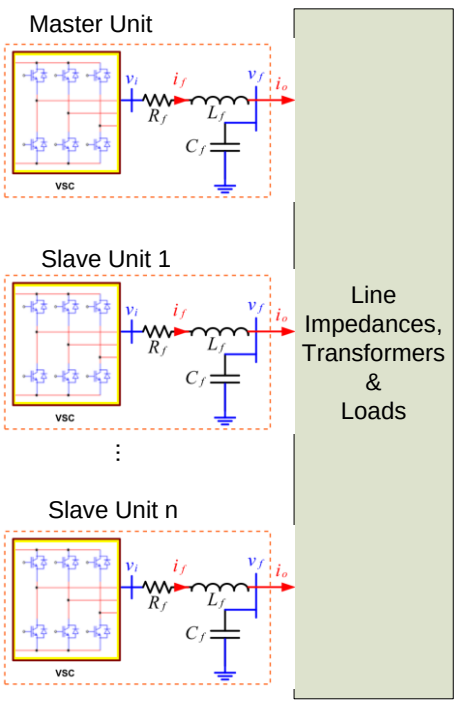

(b)

Fig. 1. Islanded MG and MS strategy, (a) A MG with two inverter-based DGs, (b) MS strategy block diagram

This MG has two inverter-based DGs and three loads; however, the models, power sharing strategy, and the designed controls can be used for any islanded MG with any number of inverter-based DGs. The DG with the larger power capacity is selected as the MU and the other as the SU. MS block diagram is illustrated in Fig. 1b. Using MS strategy, the voltage (amplitude, and frequency) is regulated by MU. In fact, MU is a grid forming inverter and it should be the largest DG. Therefore, it can obtain its energy from any source including, photovoltaic. However, to achieve maximum power point tracking (MPPT), it's better to use photovoltaic power sources as SUs (grid following units), because the active/reactive powers of SUs are controlled and MPPT can be implemented easily.

Fig. 2 illustrates an inverter-based DG unit connected to an LC filter. The state space equations in stationary reference frame for the system shown in Fig. 2 can be written as follows [15]

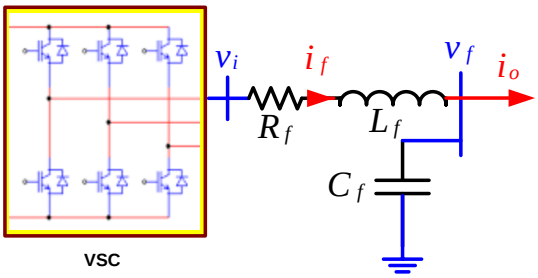

Fig. 2. An inverter-based DG unit

$$di_f/dt = a(v_i - bi_f - v_f) + \xi_i \quad (1)$$
$$dv_f/dt = c(i_f - i_o) + \xi_v \quad (2)$$

where $i_f = [i_{f\alpha}\ i_{f\beta}]^T$, $i_o = [i_{o\alpha}\ i_{o\beta}]^T$, $v_i = [v_{i\alpha}\ v_{i\beta}]^T$, $v_f = [v_{f\alpha}\ v_{f\beta}]^T$, $a = 1/L_f$, $b = R_f$ and $c = 1/C_f$. $\xi_i = [\xi_{i\alpha}\ \xi_{i\beta}]^T$, and $\xi_v = [\xi_{v\alpha}\ \xi_{v\beta}]^T$ are lumped uncertainties:

$$\xi_i = \Delta a(v_i - bi_f - v_f) - (a + \Delta a)\Delta b i_f \quad (3)$$
$$\xi_v = \Delta c(i_f - i_o) \quad (4)$$

where Δa, Δb and Δc are parameters uncertainties.

The powers injected into the filter bus are obtained as [15]

$$P = \frac{3}{2}(v_{f\alpha}i_{f\alpha} + v_{f\beta}i_{f\beta}) \quad (5)$$
$$Q = \frac{3}{2}(v_{f\beta}i_{f\alpha} - v_{f\alpha}i_{f\beta}) \quad (6)$$

The active and reactive powers are nonlinear functions of the state variables.

III. Controllers design

In this section, first, the design of an AIOFLC for a class of nonlinear systems based on the Lyapunov function is discussed, followed by employing this control design for MU and SUs.

A. AIOFLC design

Consider the following nonlinear system [22],

$$\dot{y} = f(x) + q\theta + g(x)u \quad (7)$$

where y is the output; x is states vector; $f(x)$, $g(x)$ and q are known vectors; u is control input; θ is the difference between actual and nominal values of parameters.

The following Lyapunov function is nominated [22],

$$V = \frac{1}{2}y^2 + \frac{1}{2}\tilde{\theta}^{\mathrm{T}}\Gamma\tilde{\theta} \quad (8)$$

where $\tilde{\theta} = \theta - \hat{\theta}$, and $\hat{\theta}$ is the estimated vector of θ; Γ is a strictly positive definite constant matrix.

Taking the time derivative of (6) and using (5), gives

$$\dot{V} = y\dot{y} + \tilde{\theta}^{\mathrm{T}}\Gamma\left(-\dot{\hat{\theta}}\right) = y(f(x) + q\theta + g(x)u) + \tilde{\theta}^{\mathrm{T}}\Gamma(-\dot{\hat{\theta}}) = y(f(x) + q\hat{\theta} + g(x)u) + \tilde{\theta}^{\mathrm{T}}(yq^{\mathrm{T}} - \Gamma\dot{\hat{\theta}}) \quad (9)$$

Considering the following control law and adaptation law, $\dot{V}$ in (7) becomes negative semi-definite [22].

$$u = \frac{1}{g(x)}(-f(x) - q\hat{\theta} - ky) \quad (10)$$

$$\dot{\hat{\theta}} = \Gamma^{-1}yq^{\mathrm{T}} \quad (11)$$

The positive definiteness of V and negative semi definiteness of $\dot{V}$ yield that y and $\tilde{\theta}$ are bounded. A sufficient condition for convergence of y to 0 is the uniformly continuousness of $\dot{V}$, which is satisfied if $\ddot{V}$ is bounded [23].

Substituting (10) and (11) in (9), yields

$$\dot{V} = -ky^2 \quad (12)$$

Taking the time derivative of (12) and using (7), gives

$$\ddot{V} = -2ky\dot{y} = -2ky(f(x) + q\theta + g(x)u) \quad (13)$$

Since y and $\tilde{\theta}$ are bounded, all of the variables and functions in right hand side of (13) are bounded. Therefore, $\ddot{V} < \infty$, which yields the convergence of y to 0.

B. AIOFLC for MU

To achieve a robust high-performance control of MU bus voltage, the AIOFLC is designed for MU. For this purpose, the dynamical equation of MU should be rewritten in the canonical form given in (7). Consider the following output

$$y = (v_f - v_f^*) + k_1(\dot{v}_f - \dot{v}_f^*) \quad (14)$$

where v_f^* is the MU bus voltage reference.

Taking the time derivative of (14) and using (1)-(4), gives

$$\dot{y} = (\dot{v}_f - \dot{v}_f^*) + k_1(\ddot{v}_f - \ddot{v}_f^*) = c(i_f - i_o) + \xi_v + k_1c[a(v_i - bi_f - v_f) + \xi_i] - k_1c\frac{di_o}{dt} - k_1\dot{\xi}_v - \dot{v}_f^* - k_1\ddot{v}_f^* \quad (15)$$

where the time derivative of ξ_v is given by

$$\dot{\xi}_v = \Delta c\left(\frac{di_f}{dt} - \frac{di_o}{dt}\right) \quad (16)$$

Substituting for $\dot{\xi}_v$ in (15), (15) can be considered in the canonical form (7) with

$$f(x) = c(i_f - i_o) + k_1ca(bi_f + v_f) - k_1c\frac{di_o}{dt} - \dot{v}_f^* - k_1\ddot{v}_f^* \quad (17)$$

$$q = [i_f - i_o + k_1\left(\frac{di_f}{dt} - \frac{di_o}{dt}\right)\ \ k_1c(v_i - bi_f - v_f)\ \ -k_1cai_f\ \ -k_1ci_f] \quad (18)$$

$$\theta^{\mathrm{T}} = [\Delta c\ \ \Delta a\ \ \Delta b\ \ \Delta a\Delta b] \quad (19)$$

$$g(x) = k_1ca \quad (20)$$

Substituting for (14), (17), (18), and (20) in the general control law and adaptation law given in (10) and (11), the AIOFLC is obtained for MU. The block diagram of the MU proposed controller is shown in Fig. 3.

C. AIOFLC for SUs

Taking the time derivative of (5) and (6) and substituting from (1)-(4), the dynamic equation of active and reactive powers is obtained as:

$$\dot{P} = f_P + u_P + \xi_P \quad (21)$$
$$\dot{Q} = f_Q + u_Q + \xi_Q \quad (22)$$

where

$$f_P = 1.5c[(i_{f\alpha} - i_{o\alpha})i_{f\alpha} + (i_{f\beta} - i_{o\beta})i_{f\beta}] - 1.5a[(bi_{f\alpha} + v_{f\alpha})v_{f\alpha} + (bi_{f\beta} + v_{f\beta})v_{f\beta}] \quad (23)$$

$$u_P = 1.5a(v_{f\alpha}v_{i\alpha} + v_{f\beta}v_{i\beta}) \quad (24)$$

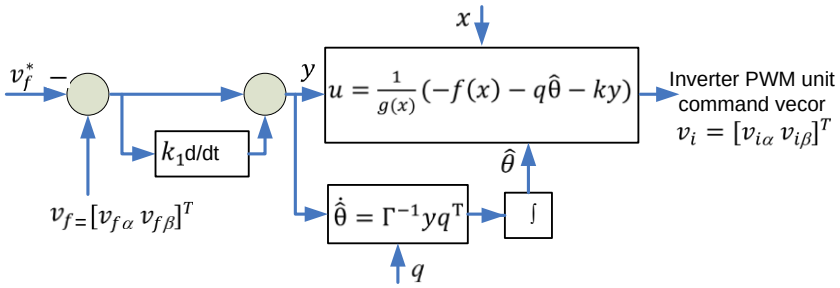

Fig. 3. Block diagram of the MU proposed controller

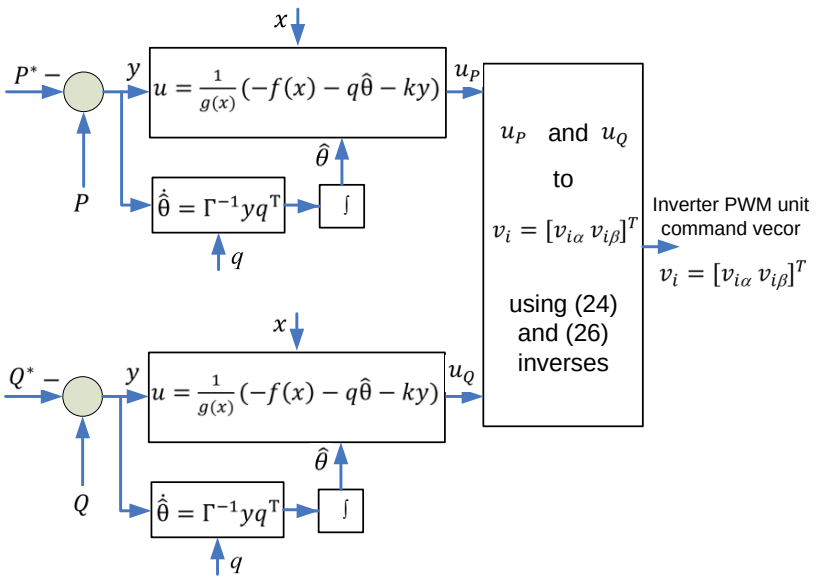

Fig. 4. Block diagram of the SUs proposed controllers

$$f_Q = 1.5c[(i_{f\beta} - i_{o\beta})i_{f\alpha} - (i_{f\alpha} - i_{o\alpha})i_{f\beta}] \quad (25)$$
$$-1.5a[(bi_{f\alpha} + v_{f\alpha})v_{f\beta} - (bi_{f\beta} + v_{f\beta})v_{f\alpha}]$$

$$u_Q = 1.5a(v_{f\beta}v_{i\alpha} - v_{f\alpha}v_{i\beta}) \quad (26)$$

ξ_P and ξ_Q are lumped uncertainties:

$$\xi_P = 1.5\xi_{v\alpha}i_{f\alpha} + 1.5\xi_{v\beta}i_{f\beta} + 1.5\xi_{i\alpha}v_{f\alpha} + 1.5\xi_{i\beta}v_{f\beta}$$
$$= \Delta c(i_{f\alpha} - i_{o\alpha})1.5i_{f\alpha} + \Delta c(i_{f\beta} - i_{o\beta})1.5i_{f\beta} + [\Delta a(v_{i\alpha} - bi_{f\alpha} - v_{f\alpha})]1.5v_{f\alpha} - (a + \Delta a)\Delta bi_{f\alpha}1.5v_{f\alpha} \quad (27)$$
$$+[\Delta a(v_{i\beta} - bi_{f\beta} - v_{f\beta})]1.5v_{f\beta} - (a + \Delta a)\Delta bi_{f\beta}1.5v_{f\beta}$$

$$\xi_Q = 1.5\xi_{v\beta}i_{f\alpha} - 1.5\xi_{v\alpha}i_{f\beta} + 1.5\xi_{i\alpha}v_{f\beta} - 1.5\xi_{i\beta}v_{f\alpha} \quad (28)$$
$$= \Delta c(i_{f\beta} - i_{o\beta})1.5i_{f\alpha} + \Delta c(i_{f\alpha} - i_{o\alpha})1.5i_{f\beta} + [\Delta a(v_{i\alpha} - bi_{f\alpha} - v_{f\alpha})]1.5v_{f\beta} - (a + \Delta a)\Delta bi_{f\alpha}1.5v_{f\beta}$$
$$+[\Delta a(v_{i\beta} - bi_{f\beta} - v_{f\beta})]1.5v_{f\alpha} - (a + \Delta a)\Delta bi_{f\beta}1.5v_{f\alpha}$$

To control the active power consider the following output

$$y = P - P^* \quad (29)$$

Taking the time derivative of (29) and using (21), gives

$$\dot{y} = f_P + u_P + \xi_P - \dot{P}^* \quad (30)$$

Considering the following functions and variables, one can achieve the canonical form (7),

$$f(x) = f_P - \dot{P}^* \quad (31)$$
$$q = [q_1\ \ q_2\ \ q_3\ \ q_4] \quad (32)$$
$$\theta^T = [\Delta c\ \ \Delta a\ \ \Delta b\ \ \Delta a\Delta b] \quad (33)$$
$$g(x) = 1 \quad (34)$$
$$u = u_P \quad (35)$$

where

$$q_1 = 1.5(i_{f\alpha} - i_{o\alpha})i_{f\alpha} + 1.5(i_{f\beta} - i_{o\beta})i_{f\beta} \quad (36)$$
$$q_2 = 1.5(v_{i\alpha} - bi_{f\alpha} - v_{f\alpha})v_{f\alpha} + 1.5(v_{i\beta} - bi_{f\beta} - v_{f\beta})v_{f\beta} \quad (37)$$
$$q_3 = -1.5ai_{f\alpha}v_{i\alpha} - 1.5ai_{f\beta}v_{f\beta} \quad (38)$$
$$q_4 = -1.5i_{f\alpha}v_{i\alpha} - 1.5i_{f\beta}v_{f\beta} \quad (39)$$

Now, the control and adaptation laws (10) and (11) can be used.

To control the reactive power, consider the following output

$$y = Q - Q^* \quad (40)$$

Taking the time derivative of (40) and using (22), gives

$$\dot{y} = f_Q + u_Q + \xi_Q - \dot{Q}^* \quad (41)$$

Considering the following functions and variables, one can achieve the canonical form (7),

$$f(x) = f_Q - \dot{Q}^* \quad (42)$$
$$q = [q_1\ \ q_2\ \ q_3\ \ q_4] \quad (43)$$
$$\theta^T = [\Delta c\ \ \Delta a\ \ \Delta b\ \ \Delta a\Delta b] \quad (44)$$
$$g(x) = 1 \quad (45)$$
$$u = u_Q \quad (46)$$

where

$$q_1 = 1.5(i_{f\beta} - i_{o\beta})i_{f\alpha} - 1.5(i_{f\alpha} - i_{o\alpha})i_{f\beta} \quad (47)$$

$$q_2 = 1.5(v_{i\alpha} - bi_{f\alpha} - v_{f\alpha})v_{f\beta} - 1.5(v_{i\beta} - bi_{f\beta} - v_{f\beta})v_{f\alpha} \quad (48)$$

$$q_3 = -1.5ai_{f\alpha}v_{i\beta} + 1.5ai_{f\beta}v_{f\alpha} \quad (49)$$

$$q_4 = -1.5i_{f\alpha}v_{i\beta} + 1.5i_{f\beta}v_{f\alpha} \quad (50)$$

Now, the control and adaptation laws (10) and (11) can be used. The block diagram of the SUs proposed controllers is shown in Fig. 4.

IV. Case studies and operation scenarios

Simulation studies are performed in MATLAB SIMULINK to investigate the designed control scheme for the MG given in Fig. 1. The parameters used in simulations are presented in Table 1. The SIMULINK solver is configured as a fixed-step with a discrete sample time of 5μs. The MU rated power and the inverters rated voltages are used as base values. The operation of the MG is evaluated using the designed controls in several cases.

A. Case Study 1

This case study is the normal testing operation for the proposed controls. In this case study, from t=0s to t=0.15s, only the MU delivers the demand powers. From t=0.15s to t=0.25s, the active power of the SU increases from 0 to 0.4pu linearly. From t=0.15s to t=0.2s, the reactive power of the SU increases from 0 to 0.1pu linearly. Fig. 5 presents the voltages and powers of three buses (i.e. PC1, PC2, and Load3) of this case study. The obtained results show the active/reactive powers track their reference values correctly. It is seen that the MU power decreases by increasing the SU power. The voltages are sinusoidal with very low harmonics and the MU bus voltage is controlled properly. No voltage deviation is observed and the responses are acceptable without any low-frequency oscillations. The voltage THDs are below the 2.5% required by IEEE 1547 and IEC 61727 standards (50% of the current harmonic limits) [24].

B. Case Study 2

In this case, all of the settings are similar to the ones given in case study 1; except that, the controllers are FLCs. Fig. 6 illustrates the obtained results of this case study. Unlike case study 1, some large oscillations are seen on active/reactive powers of MU and Load3 which are the consequences of the noticeable increases and decreases in voltages. In fact, using FLC, the MU voltage tracking is not as good as the tracking in case study 1. Besides, FLC is not a robust control against disturbances and uncertainties.

C. Case Study 3

In this case study, again all of the settings are similar to the ones considered in case 1, but the applied controls are modified CSMCs. The simulation results of this case study are shown in Fig. 7. The chattering effect and high control efforts are very noticeable. The active/reactive powers are affected really and contain high-frequency contents. VSIs filters cannot eliminate these high-frequency contents completely. The chattering phenomena can also excite unmolded dynamics which may cause instability in the real physical system. Besides, it increases the power loss of VSI switches.

TABLE 1
MG PARAMETERS

The nominal (base) power	3 MVA
VSIs nominal voltage	600 V
MG frequency	50 Hz
Line1	0.35+j0.785 Ω
Line2	0.25+j0.625 Ω
Line3	0.1+j0 Ω
VSIs DC voltage	1500 V
Switching frequency	2 kHz
Filter resistance	0.002 Ω
Filter inductance	500 μH
Filter capacitance	400 μF

The control signals of the three controllers are also shown in Figs. 3, 4, and 5. These waveforms illustrate the lower control effort of the AIOFLC.

D. Case Study 4

Nonlinear and switching loads such as rectifiers increase harmonic distortions in the power system. This case study is fully identical to case study 1, except that a rectifier, which is a nonlinear load, is paralleled to Load3 at time 0.35s. Fig. 8 shows the obtained results of this case study. Using the proposed AIOFLCs reveals that despite the harmonics in Line3 current, the voltages remain sinusoidal, and MU and SU provide the demand powers without any considerable glitch. Using the AIOFLCs, the MG has a smooth and acceptable operation. The effect of harmonic load on voltages and powers is insignificant due to the proposed high-performance controls. This case study also illustrates the robustness of the designed AIOFLCs.

E. Case Study 5

This case is fully similar to case 1; however, very higher impedances are used for Line1 and Line2: (0.35+j0.785)*6 Ω and (0.25+j0.625)*6 Ω, respectively. Fig. 9 illustrates the obtained results of this case study. The simulation results show that the MG maintains its stability; however, the harmonic contents of bus voltages are very high and the active/reactive powers are very fluctuating. This test represents that the MS strategy is only acceptable for islanded MGs in which the impedances of the lines are not very high. It can also be used in power electronics systems with paralleled VSIs.

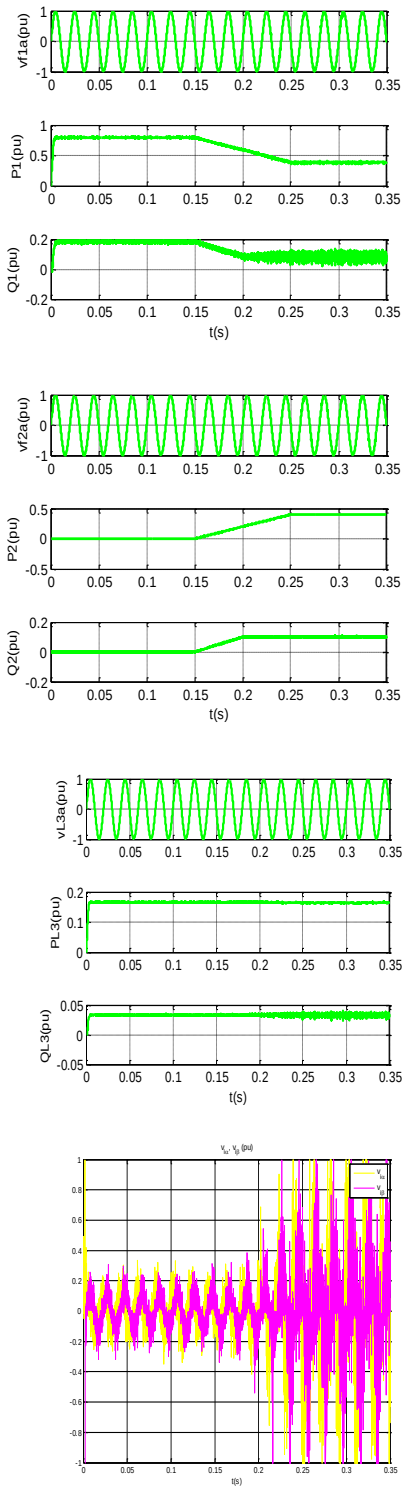

Fig. 5. AIOFLC: voltage, active/reactive powers of buses, and control signals of DG1

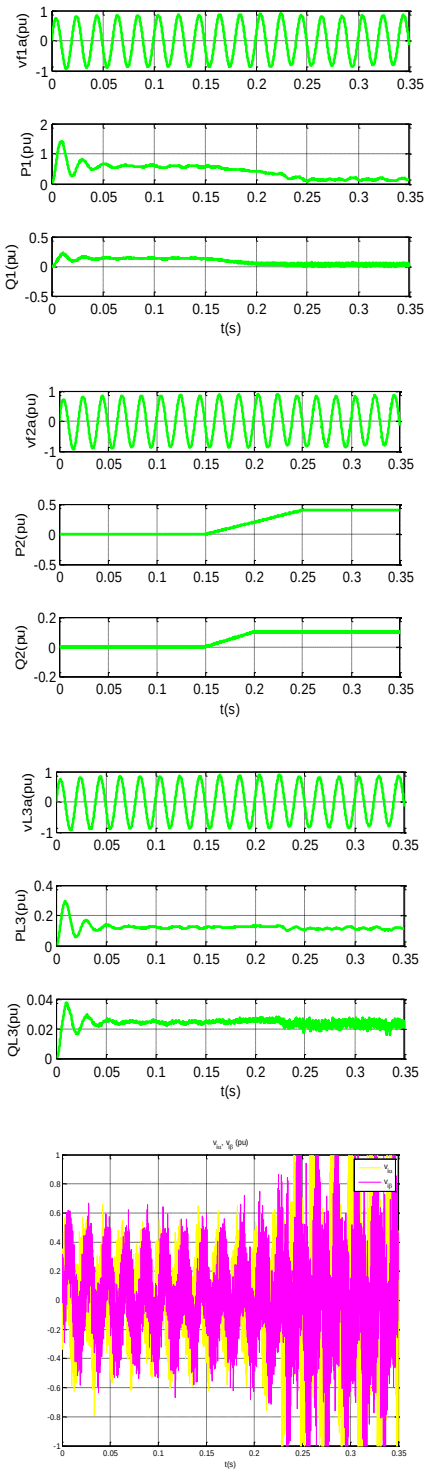

Fig. 6. FLC: voltage, active/reactive powers of buses, and control signals of DG1

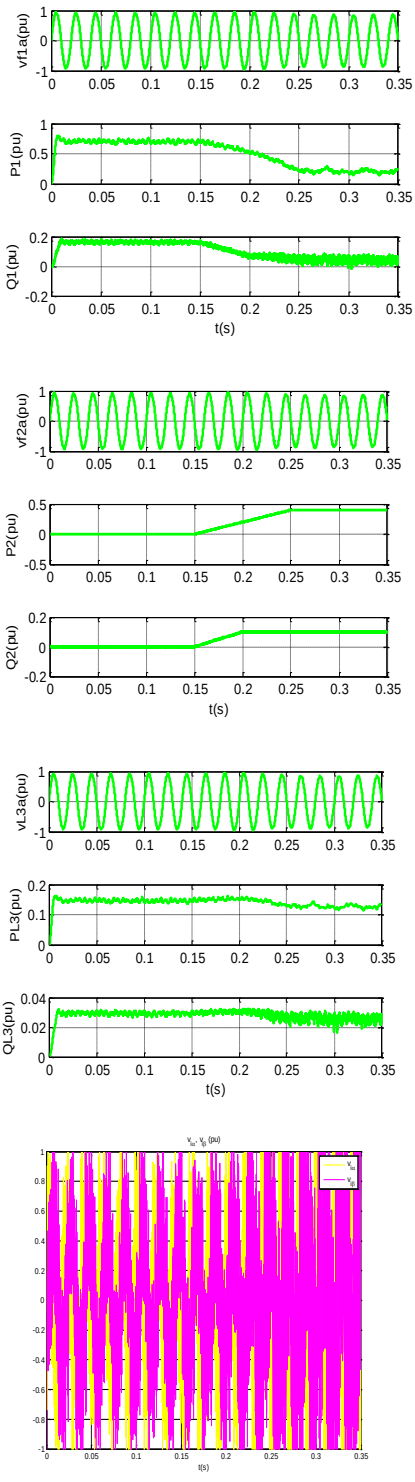

Fig. 7. Modified CSMC: voltage, active/reactive powers of buses, and control signals of DG1

F. Case Study 6

In this case study, using the parameters of case studies 1 to 3, the load switching is studied. Load2 on bus2 is disconnected at 0.3 second and connected again at 0.4 second. The simulation results of the proposed AIOFLC are represented in Fig. 10 and compared to the ones of two other standard nonlinear control methods. It is seen that using AIOFLC, the active/reactive powers of DG2 are controlled with fewer ripples, and the active/reactive powers of DG1 are also properly changed according to the load variations.

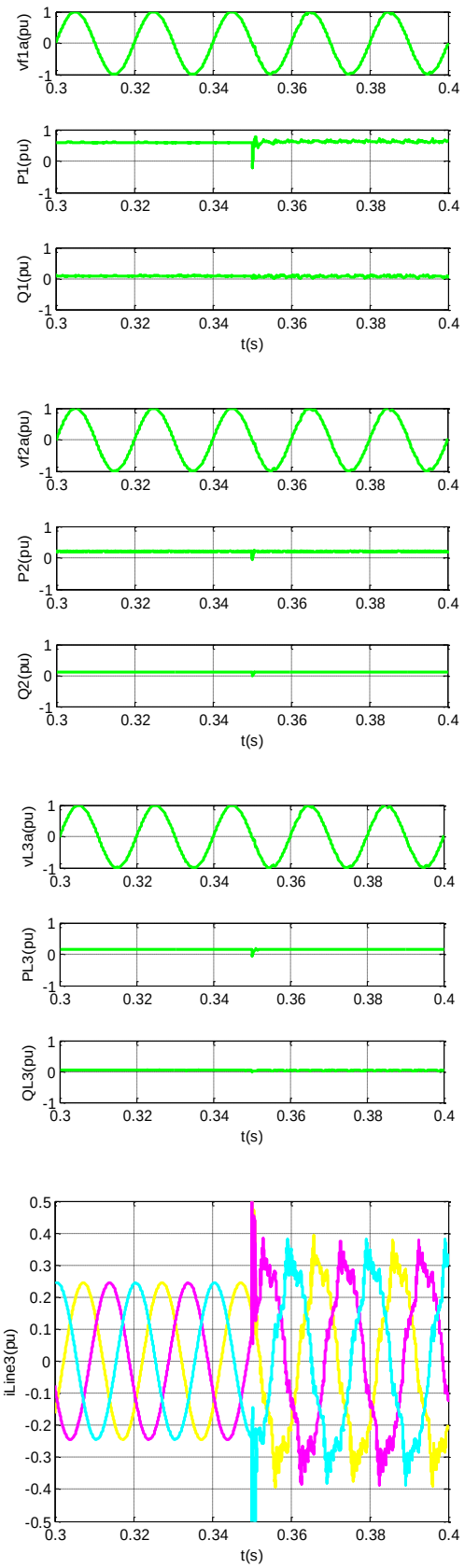

Fig. 8. AIOFLC with harmonic load (rectifier): voltage, active/reactive powers of buses, currents of the Line3

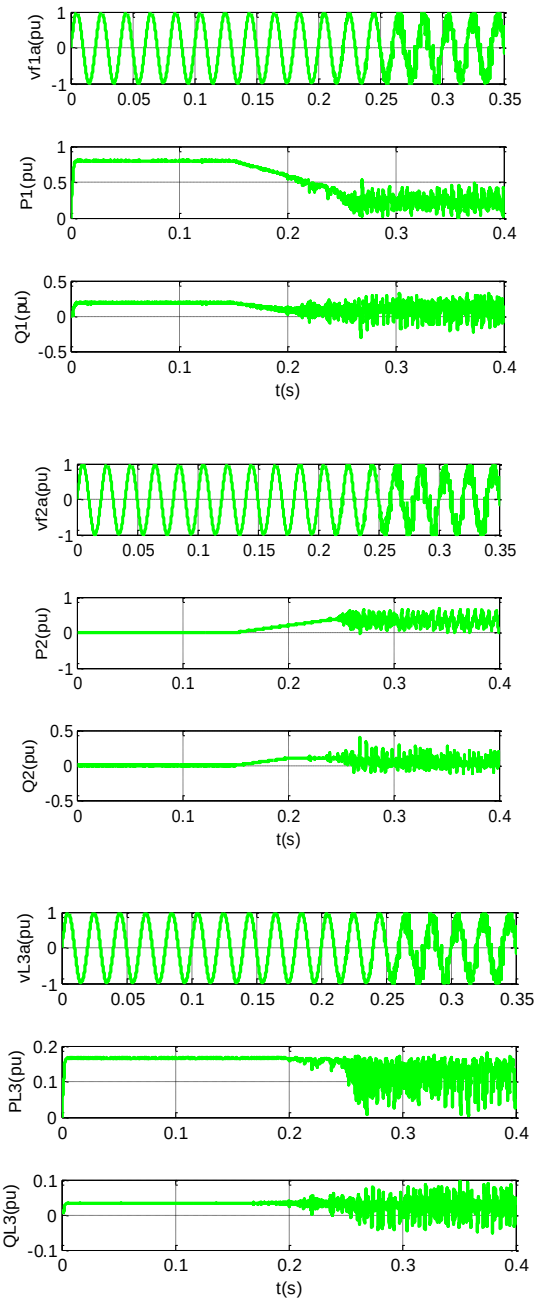

Fig. 9. High impedance lines: voltage, active/reactive powers of buses

V. Conclusions

This paper investigates AIOFLC to control islanded inverter-based MGs with MS strategy. Two AIOFLCs are designed for MU and SUs. Simulation results are obtained for an islanded MG with two DGs; however, the proposed controls can be used well for any islanded inverter-based MG with any number of DGs. Next, the responses of three controls (i.e., AIOFLC, FLC, and a modified CSMC) are obtained and compared. The obtained results illustrate the benefits of the designed

AIOFLCs. The MU bus voltage and the delivered powers of the SU are controlled properly.

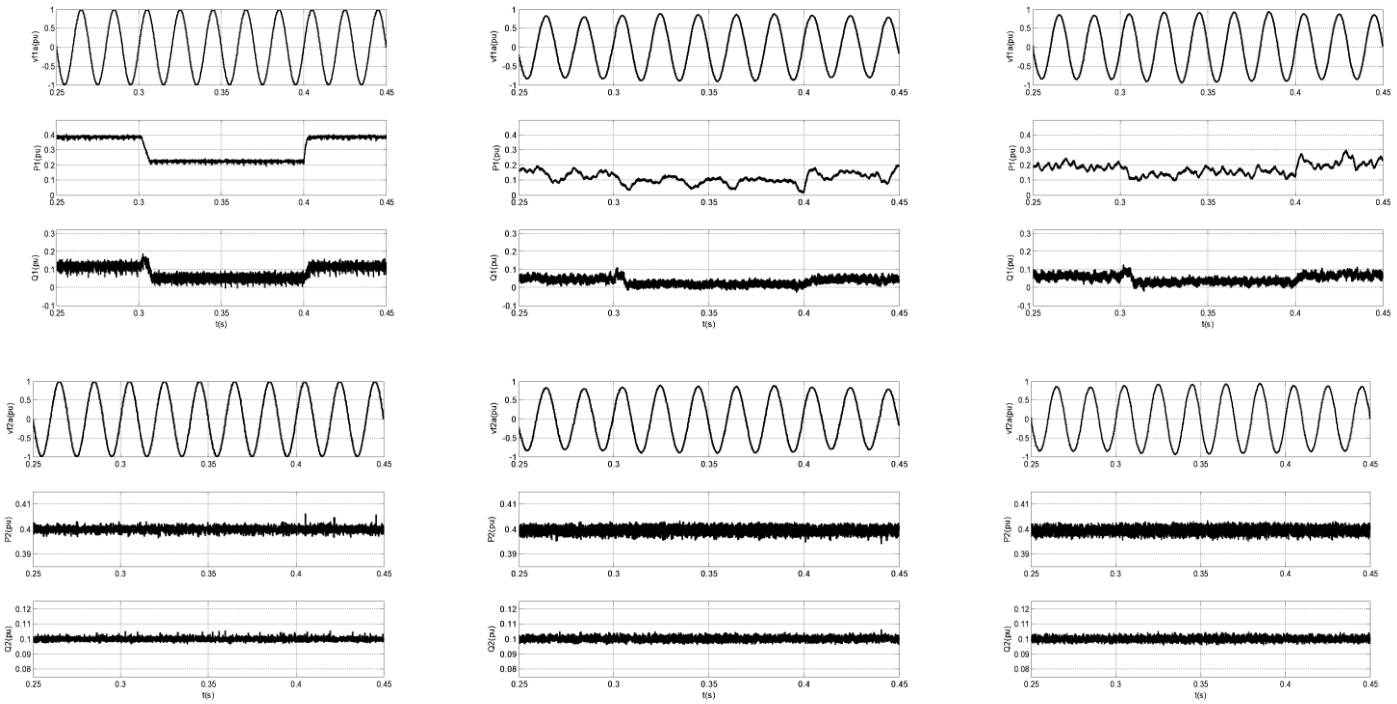

(a) (b) (c)

Fig. 10. Load switching: voltage, active/reactive powers of buses 1&2, (a) AIOFL, (b) FLC, (c) CSMC

By changing the loads or the active/reactive powers references of the SU, the MU generates the remaining load demand and a proper load sharing between VSIs is achieved. Using the proposed control scheme leads to almost no overvoltage or undervoltage during the transient intervals. The designed controllers provide a high-performance control behavior. In addition, simulating the volatility inherent to the DGs illustrates that the DGs can inject their powers when available. Overall, the merits of the proposed control scheme are as follows: perfect tracking, avoiding high control effort, and robustness of the AIOFLCs. The designed AIOFLCs can be used in parallel inverters with LC filters to control the voltage and power. The contributions of the paper can be summarized as follows:

- Rearranging the equations of inverter-based DGs with LC filters, suitable for controller design
- Designing two AIOFLCs for the MU and the SUs
- Investigating the proposed controls in a MG by adopting the MS strategy

REFERENCES

[1] A. Alfergani, A. Khalil, "Modeling and Control of Master-Slave Microgrid with Communication Delay," The 8 th International Renewable Energy Congress (IREC 2017), 2017.

[2] J. Pinto, A. Carvalho, V. Morais, "Power Sharing in Island Microgrids," Frontiers in Energy Research, Vol. 8, Article 609218, pp. 1-14, 2021.

[3] P. J. dos Santos Neto, T. A.S. Barros, J. P.C. Silveira, E. R. Filho, J. C. Vasquez, J. M. Guerrero, "Power management techniques for grid-connected DC microgrids: A comparative evaluation," Applied Energy,269, 115057, pp. 1-15, 2020.

[4] M. Hamzeh, H. Karimi, H. Mokhtari, "A New Control Strategy for a Multi-Bus MV Microgrid Under Unbalanced Conditions," IEEE Trans. On Power Systems, Vol. 27, No. 4, pp. 2225-2232, Nov. 2012.

[5] H. Han, X. Hou, J. Yang, J. Wu, M. Su, J. M. Guerrero, "Review of Power Sharing Control Strategies for Islanding Operation of AC Microgrids," IEEE Trans. On Smart Grid, pp. 1-16, 2015.

[6] G. B. Narejo, B. Acharya, R. S. S. Singh, and F. Newagy, Microgrids Design, Challenges, and Prospects, Taylor & Francis Group, LLC, 2022.

[7] T. Caldognetto, P. Tenti, "Microgrids Operation Based on Master-Slave Cooperative Control," IEEE Journal of Emerging and Selected Topics in Power Electronics, Vol. 2, No. 4, pp. 1081 – 1088, 2014.

[8] M. S. Mahmoud , O. Al-Buraiki , "Two-level Control for

Improving the Performance of MicroGrid in Islanded Mode," 2014 IEEE 23rd International Symposium on Industrial Electronics (ISIE), Istanbul, Turkey, pp. 54-59, 2014.

[9] P. Monshizadeh, C. De Persis, N. Monshizadeh, A. V. D. Schaft, "A Communication-Free Master-Slave Microgrid with Power Sharing," 2016 American Control Conference (ACC), Boston, USA, 2016.

[10] H. Liang, Y. Dong, Y. Huang, C. Zheng, P. Li, "Modeling of Multiple Master–Slave Control under Island Microgrid and Stability Analysis Based on Control Parameter Configuration," Energies, Vol. 11, No. 9, pp. 1-18, 2018.

[11] J. Marchgraber, W. Gawlik, "Investigation of Black-Starting and Islanding Capabilities of a Battery Energy Storage System Supplying a Microgrid Consisting of Wind Turbines, Impedance- and Motor-Loads," Energies, Vol. 13, No. 19, pp. 1-24, 2020.

[12] T. Yao, R. Ayyanar , "Variable Structure Robust Voltage Regulator Design for Microgrid Master-Slave Control," 2017 IEEE Energy Conversion Congress and Exposition (ECCE), Cincinnati, OH, USA, 2017.

[13] M. Babazadeh and Houshang Karimi, "Robust Decentralized Control for Islanded Operation of a Microgrid," 2011 IEEE Power and Energy Society General Meeting, Detroit, MI, USA, 2011.

[14] M. Dehghani,T. Niknam, M. Ghiasi, H. Baghaee, F. Blaabjerg, T. Dragicevĭć and M. Rashidi, "Adaptive backstepping control for master-slave AC microgrid in smart island," Energy, Vol. 246, 2022.

[15] M. M. Rezaei, J. Soltani, "Robust control of an islanded multi-bus microgrid based on input – output feedback linearisation and sliding mode control," IET Generation, Transmission & Distribution, Vol. 9, No. 15, pp. 2447–2454, 2015.

[16] M. Cucuzzella, G. P. Incremona, A. Ferrara, "Design of Robust Higher Order Sliding Mode Control for Microgrids," IEEE Journal on Emerging and Selected Topics in Circuits and Systems, Vol. 5, No. 3, pp. 393-401, 2015.

[17] J. Wang, .Z. Liu, J. Liu, T. Wu, "A Mode Switching-Based Decentralized Secondary Control for Microgrids With Hybrid Droop and Master-Slave Structure," IEEE Open Journal of Power Electronics, Vol. 3, pp. 334-347, 2022.

[18] F. Carnielutti, M. Aly, M. Norambuena, J. Rodriguez, "Model Predictive Control for Master-Slave Inverters in Microgrids," IECON 2022 – 48th Annual Conference of the IEEE Industrial Electronics Society, Brussels, Belgium, 2022.

[19] S. Shajari, R. Keypour, "A New Enhanced Droop Controller for Seamless Load Sharing in AC Microgrids in Presence of Wind Turbine and Photovoltaic Sources," International Journal of Industrial Electronics, Control and Optimization, Vol. 5, No. 2, pp. 153-165, April 2022.

[20] M. Alizadeh, H. Askarian, A. Bakhshai, N. Khodabakhshi-Javinani, "An Enhanced Distributed State Feedback for Secondary Control in an Islanded Microgrid," International Journal of Industrial Electronics, Control and Optimization, Vol. 5, No. 2, pp. 123-132, April 2022.

[21] N. R. Abjadi, "Nonsingular Terminal Sliding Mode Control for Islanded Inverter-Based Microgrids," Journal of Operation and Automation in Power Engineering, Vol. 12, No. 1, pp. 26-34, Jan. 2024.

[22] S. A. A. Fallahzadeh, N. R. Abjadi, A. Kargar, "Decoupled Active and Reactive Power Control of a Grid-Connected Inverter-Based DG Using Adaptive Input–Output Feedback Linearization," Iranian Journal of Science and Technology, Transactions of Electrical Engineering, 2020.

[23] Z. Ding, Nonlinear and Adaptive Control Systems, Published by The Institution of Engineering and Technology, London, United Kingdom, 2013.

[24] R. Teodorescu, M. Liserre, P. Rodriguez, Grid Converters for Photovoltaic and Wind Power Systems, John Wiley & Sons, Ltd, United Kingdom, 2011.

Navid Reza Abjadi received the B.S., M.S., and Ph.D. degrees in electrical engineering from Isfahan University of Technology, Isfahan, Iran in 1999, 2001, and 2010 respectively. He is a lecturer at Shahrekord University. His research interests include motor drives, control theory applications, and power electronics.